Biosensors and Bioelectronics 79 (2016) 251–257

Contents lists available at ScienceDirect

Biosensors and Bioelectronics

journal homepage: www.elsevier.com/locate/bios

Impedance spectroscopy analysis of human odorant binding proteins immobilized on nanopore arrays for biochemical detection

Yanli Lu [a], Diming Zhang [a], Qian Zhang [a], Yixuan Huang [a], Senbiao Luo [b], Yao Yao [a], Shuang Li [a], Qingjun Liu [a,*]

[a] Biosensor National Special Laboratory, Key Laboratory for Biomedical Engineering of Education Ministry, Department of Biomedical Engineering, Zhejiang University, Hangzhou 310027, PR China
[b] Shangyu People's Hospital of Zhejiang Province, Shangyu 312000, PR China

ARTICLE INFO

Article history:
Received 17 September 2015
Received in revised form
13 December 2015
Accepted 14 December 2015
Available online 17 December 2015

Keywords:
Human odorant binding protein (hOBPs)
Impedance spectroscopy
Nanopore array
Biosensor
Biochemical detection

ABSTRACT

Human odorant-binding proteins (hOBPs) not only can bind and transport odorants in the surrounding environment for sensing smells, but also play important roles in transmitting lots of biomolecules in different organs. Utilizing the properties of hOBPs, an electrochemical biosensor with nanopore array was developed to detect specific biomolecular ligands, such as aldehydes and fatty acids. The highly ordered nanopores of anodic aluminum oxide with diameter of 20–40 nm were fabricated with two-step oxidation. Through 2-carboxyethyl phosphonic acid, hOBPs were self-assembled on nanopores as the sensing membrane. With nanopore arrays, the impedance spectra showed quite different electron transfer processes in the frequency spectra, which could be characterized by the electron transfer resistance and electrical resistance of the porous membrane. Under stimulation of biomolecular ligands, series resistance of nanopores and hOBPs increased and showed a concentration-dependence feature, while the electron transfer resistance hardly changed. The nanopore based biosensor could sensitively detect biological ligands of benzaldehyde, docosahexaenoic acid, and lauric acid, which were closely related to or were potential biomarkers for cancers and other serious diseases. Equipped with hOBPs, the sensor exhibited promising potentials both in odorant and biomolecule detection for olfactory biosensing and in disease diagnosis and evaluation for biochemical detection.

1. Introduction

As one of the most ancient forms of senses, olfaction of human beings not only can discriminate different objects and interpret various environments in real time, but also plays vital roles in enhancing our life quality (Stevenson, 2010; Semin and De Groot, 2013). It starts with odorants acquisition or sniffing, which is followed by transduction at the sensory neurons that line in the olfactory epithelium. In order to reach and trigger respective ORs embedded in cell membrane, however, odorants that are generally hydrophobic molecules should be firstly conveyed through the aqueous nasal mucus. The solubilizers and carriers of odorants of human beings are low-molecular-weight soluble proteins that are called human odorant-binding proteins (hOBPs), which were abundantly secreted in the olfactory apparatus (Tegoni et al., 2000; Charlier et al., 2009).

Except for sensitively binding chemical cues, hOBPs share a universal tertiary structure of odorant-binding proteins (OBPs), which was characterized by a hydrophobic cavity, "calyx" (Lescop et al., 2009; Schiefner and Skerra, 2015). Depending on the substantial conformational plasticity of the calyx, hOBPs could accommodate numerous lipophilic molecules of diverse chemical structures. Moreover, hOBPs have higher affinities for aldehydes and fatty acids (Tcatchoff et al., 2006). They were treated not only as important odorants, but also as vital biomolecules or even biomarkers that have very close relationships with gastrointestinal disease, angiocardiopathy, and even cancers (Garner et al., 2007; Bougnoux et al., 2010; Du et al., 2015). Structural biology and synthetic biology have found that they were robust enough to stand up to wide ranges of pH and temperatures (even to 80–100 °C), for substantial mistreatments (Hou et al., 2005; Wei et al., 2008). Additionally, OBPs were easier to be isolated and purified in the process of production when compared with membrane protein of receptors, which have seven transmembrane α-helixes (Kaiser et al., 2008). All of these suggested that as the first sensing filter of human olfaction, hOBPs based systems will provide good opportunities to best approximate the natural mechanisms of olfaction to mimicking the human smells directly.

* Corresponding author.
E-mail address: qjliu@zju.edu.cn (Q. Liu).

http://dx.doi.org/10.1016/j.bios.2015.12.047
0956-5663/

Combined with different bio-recognition elements, such as proteins and ssDNA, nanopore-based devices have fabricated protein biosensing and even single molecule detection (Stoloff and Wanunu, 2013; Makra and Gyurcsányi, 2014). More importantly, using solid-state nanopores functionalized with proteins or peptides that would induce conformational changes by the corresponding testing substances, the detection signals could be greatly amplified (Wei et al., 2012; Liebes-Peer et al., 2014). Taking advantage of the nanoscale holes that the only connection for ions and fluid be transferred between the two parts of nanopore devices, electrochemical testing, such as electric current and impedance spectroscopy was widely studied, because of the good stability and no fluorescent labels during the measurement (Schoch et al., 2008; Santos et al., 2013).

Previous studies suggested that interactions between OBPs and their ligands could be sensitively detected by electrochemical impedance with insect proteins immobilized on the electrodes (Liu et al., 2013; Lu et al., 2015), which inspired us that nanopore-based devices functionalized with hOBPs might have potentials in sensing different ligands, including odorants, and even other important lipophilic biomolecular ligands. Herein we have sought to utilize the binding properties of hOBPs to develop biosensors for biomolecule detection. With highly ordered nanopores, an electrochemical biosensor was established to interpret interactions between hOBPs and different ligands, such as disease related aldehydes and fatty acids. As a sensitive and specific method to detect different biomolecules, this impedance biosensor showed promising potentials in odorant sensing, human olfaction investigation, biochemical detection, and disease diagnostics.

2. Experiment

2.1. Recombinant hOBP and reagents

The expression and purification of the active recombinant hOBP were cloned from the full-length cDNA of human in Sino Biological Inc. (China). Briefly, a DNA sequence encoding the hOBP was expressed with a polyhistidine tag at the C-terminus in the host cells of human. After harvesting the host cells, the crude cell extracts, pellet and supernatant were analyzed by sodium dodecyl sulfate-polyacrylamide gel electrophoresis (SDS-PAGE). The recombinant hOBP consisted of 166 amino acids and predicted a molecular mass of 19.4 kDa. The protein was resuspended (20 μg/ml) in phosphate buffered saline (PBS; pH = 7.4) and saved under 4 °C for the following experiments.

The solvents and reagents, 1-ethyl-3-(3-dimethylaminopropyl) carbodiimide (EDC), N-hydroxysuccinimide (NHS), potassium ferricyanide/ferrocyanide $K_4[Fe(CN)_6]/K_3[Fe(CN)_6]$, phosphate buffered saline (PBS), 2-(4-Morpholino) ethanesulfonic acid (MES), 2-carboxyethyl phosphonic acid, docosahexaenoic acid, lauric acid, and benzaldehyde for protein immobilization and impedance detection were all purchased from Sigma-Aldrich, USA.

2.2. Nanopores and biosensor setup

Anodic aluminum oxide nanopore arrays were prepared by the two-step anodization in LeSen nano science and technology co., Ltd. (China). Briefly, the first anodization process has been taken in 0.25 M oxalic acid. Then, the aluminum was etched in chromic acid and phosphoric acid. The second anodization step was repeated in 0.25 M oxalic acid. The detailed fabrication process was in the Appendix (Fig. A1). Finally, about 5–10 μm thick, free standing nanopores with uniform pore diameters of 20–40 nm were fabricated (Fig. 1a).

The experimental apparatus is illustrated in Fig. 1b. A piece of nanopore membrane with an active area of 3 mm^2 was placed in the middle of two equal chambers. Both chambers were filled with 200 μl, 10 mM $[Fe(CN)_6]^{3-/4-}$, which was selected to indicate the efficiency of ion blockage. The electrochemical impedance spectroscopy measurements were performed using CH Instruments 660E electrochemical analyzer (CH Instruments, Inc.) with

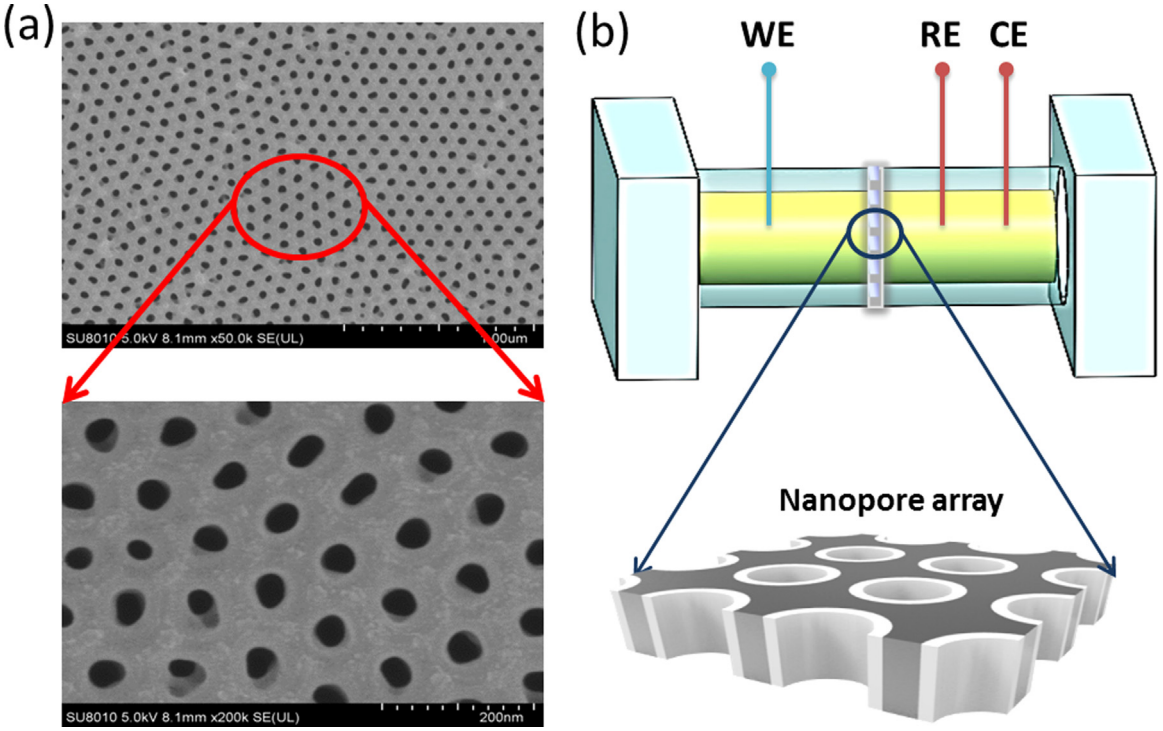

Fig. 1. Schematic of the electrochemical hOBPs biosensor system: (a) SEM image of nanopores in top view and (b) experimental setup with nanopore arrays (WE: working electrode; RE: reference electrode; CE: counter electrode).

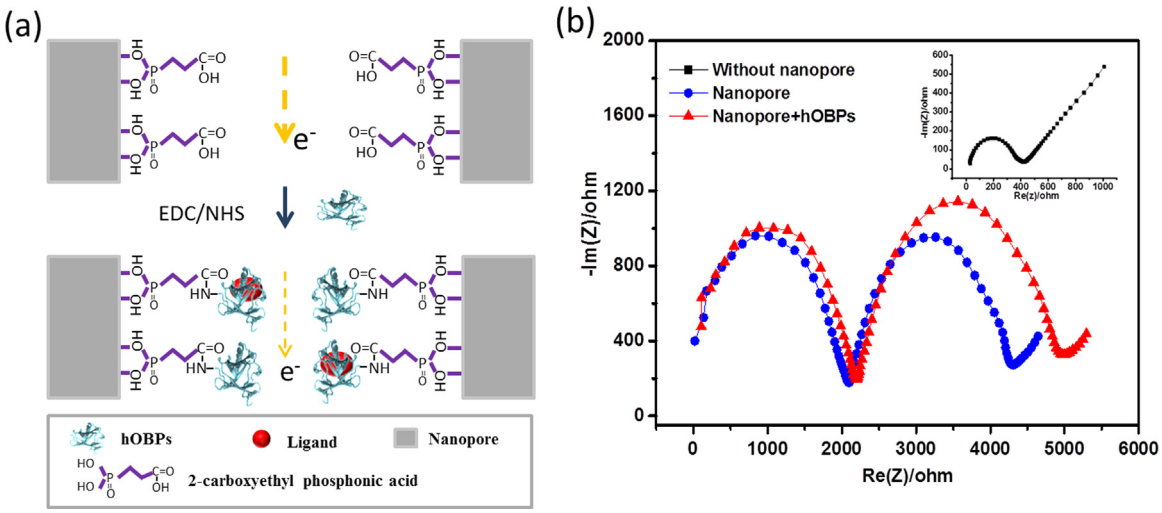

Fig. 2. Immobilization of hOBPs on nanopores: (a) hOBPs immobilized on nanopores with 2-carboxyethyl phosphonic acid via EDC/NHS coupling. (b) Impedance spectra of hOBPs immobilized on nanopores. (The blank line with squares: three-electrode system without nanopores, the red line with triangles: three-electrode system with nanopores, the blue line with circles: hOBPs immobilized on nanopores.) (For interpretation of the references to color in this figure legend, the reader is referred to the web version of this article.)

electrodes of gold working electrode, silver–silver chloride reference electrode and platinum counter electrode, immersed in the electrolyte solution of both chambers, respectively.

2.3. Immobilization of hOBPs

Firstly, nanopores were thoroughly rinsed with ethanol and ultrapure water to remove the organic residues off the substrate. Subsequently, the nanopores were soaked in an aqueous solution of 5 mM 2-carboxyethyl phosphonic acid for 72 h for modification (Kant et al., 2014). The two hydroxyl functional groups of 2-carboxyethyl phosphonic acid could form P–OH with nanopores, while the carboxylic groups could offer binding sites for proteins through amido bonds (Fig. 2a).

After rinsing with a sufficient amount of ultrapure water and drying in nitrogen, the modified nanopore arrays were used to immobilize protein via EDC/NHS coupling. EDC and NHS solutions were prepared in 0.1 M MES buffer (pH=5, contained 0.5 M NaCl) and 0.1 M PBS buffer (pH=7.4) respectively. Equal volume of EDC (8 mg/ml) and NHS (16 mg/ml) solutions, 50 µl, was successively added into nanopores to activate the carboxyl groups for 15 min. After pH was increased from 7.2 to 7.5 with sodium bicarbonate, 50 µl of hOBPs solution was also added. Finally, the solution in the plate well was mixed by an oscillator for about 2 min and incubated them for 2 h to allow forming the amide linkages (Fig. 2a). Then, after rinsing with PBS buffer to remove the unreacted EDC/NHS solutions and unbound proteins, the device with immobilized hOBPs was saved under 4 °C. All of the above immobilizing processes were performed at room temperature (22 ± 2 °C).

2.4. Ligands sensing with the impedance spectroscopy

The tested aldehydes and fatty acids, benzaldehyde, lauric acid, and docosahexaenoic acid were used as the sensing biomolecular ligands. Taking methanol as solvent, these ligands were prepared for different concentrations, 10^{-8} mg/ml, 10^{-7} mg/ml, 10^{-6} mg/ml, 10^{-5} mg/ml, and 10^{-4} mg/ml. The ligands of different concentrations, 100 µl, were added to the two chambers containing 100 µl $Fe[CN)_6]^{3-/4-}$ (1:1) respectively for recording the electrochemical impedance spectroscopy, as the tested frequencies were set from 1 Hz to 1 MHz with 5 mV alternating voltage.

After each measurement, the tested solutions were removed out of the plate wells, and 400 µl PBS was added to soak the nanopore arrays for 10 min to eliminate the residual ligands for the recovery of the proteins (Appendix, Fig. A2). Parallel experiments for each ligand were tested at least three times. All of the impedance detections were also performed at room temperature (22 ± 2 °C). In the data analysis, characteristic resistances of each impedance spectrum were extracted to calculate the normalized impedance changes of different ligands, which was described as $(Z_b - Z_a)/Z_b$, where Z_b and Z_a represent half of the characteristic resistances before and after the ligand stimulation respectively.

3. Results

3.1. hOBPs functionalized nanopore arrays

Electrochemical impedance is a powerful analytical method that has been used for a wide range of applications from chemical analysis to biological monitoring. Generally, the impedance spectrum of the three-electrode system contains two portions, a semicircle at high frequencies that represented electron transfer process, and a straight line at lower frequencies that mainly represented electronic diffusion process. The tested impedance spectrum without nanopores shared the same features with the theoretical result (Fig. 2b). The diameter of the semicircle in the impedance spectrum was equal to the charge transfer resistance, which was often extracted as the characteristic resistance. However, when the nanopores were placed between the working electrode and reference/counter electrodes, they had a great influence to the whole impedance spectra.

Comparing the impedance spectra of the three-electrode system with and without nanopores, it could be inferred that nanopores strongly affect the electrochemical process, not only by increasing the charge transfer resistance, but also by introducing additional electron transfer process (Figs. 2 and A2). Moreover, the immobilization of hOBPs on self-assembled nanopores led these two electron transfer processes more difficult, especially that introduced by nanopores. It could be reflected by the increasing characteristic resistances. Therefore, impedance of the hOBPs functionalized nanopores was greatly influenced by nanopores and hOBPs, which might be caused by changing the dielectric features of the nanopores and nanopore/electrolyte interface. The

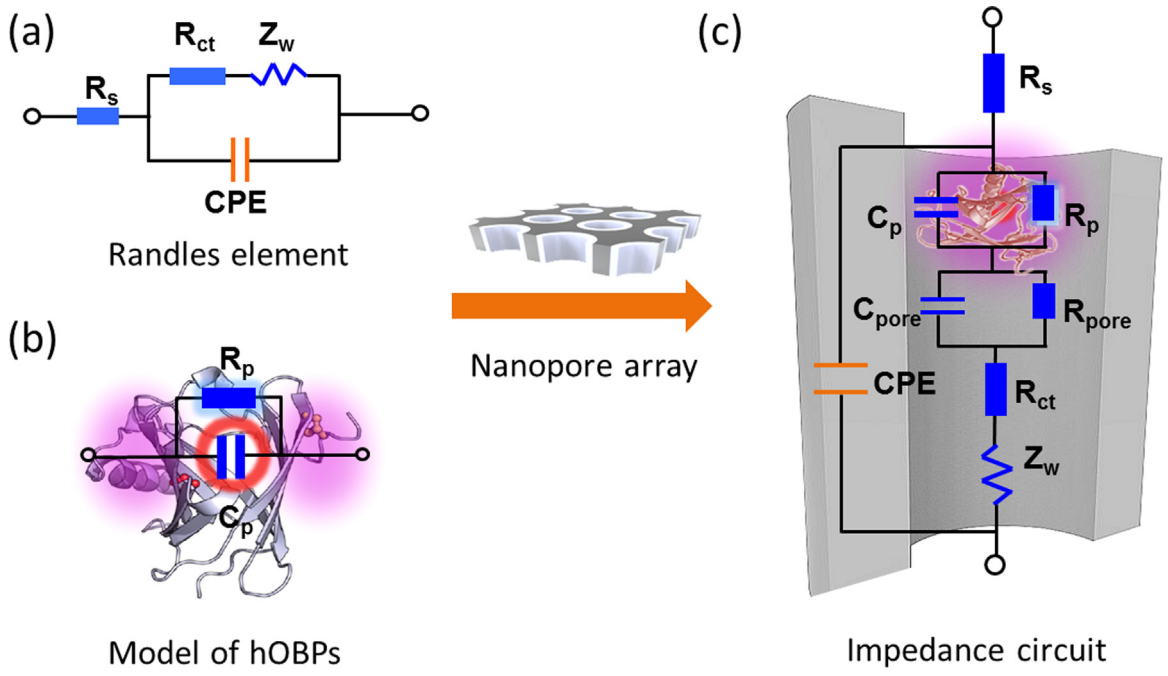

Fig. 3. The electrical properties and the theoretical impedance model of hOBPs functionalized nanopore arrays: (a) Randle element for electrochemical impedance; (b) cartoon of the protein backbone and cavity with the equivalent circuit; and (c) equivalent circuit of hOBPs functionalized nanopores.

impedance changes also suggested that hOBPs have been successfully immobilized on the nanopore arrays for ligand detections.

Usually, the impedance spectrum could be analyzed by the Randles circuit, with solution resistance (R_s), charge transfer resistance (R_{ct}), warburge impedance (Z_w), and constant phase element (*CPE*), as shown in Fig. 3a (Lisdat and Schäfer, 2008). R_s and Z_w represent bulk properties of the electrolyte solution. *CPE* and R_{ct} both depend on the dielectric and insulting features at the electrode/electrolyte interface that were often affected by the property changes occurring at the electrode interface. When aluminum oxide was made into nanoporous anodic aluminum oxide, the resistance decreased a lot because of nanoscale pores. However, for small pores with diameters smaller than 100 nm, the nanopore resistance R_{pore} was usually larger than the solution resistance R_s, which might play an important role in the impedance sensing (Albrecht, 2011; Vitarelli and Talaga, 2013). Additionally, electrolyte around the nanopores could also bring a capacitance C_{pore} due to positive and negative charges on the surface of aluminum oxide. Both R_{pore} and C_{pore} were used to represent the impedance properties of nanopores.

In impedance sensing, electrical properties of protein could be treated as a resistance–capacitance parallel circuit on the electrodes (Lu et al., 2014). To hOBPs of this study, the backbone structure that was made up by 8-stranded β-barrel and one α-helix could be represented by a resistance (R_p), while the predominantly hydrophobic internal cavity was equivalent to a capacitance (C_p), as shown in Fig. 3b. Therefore, from the impedance spectra of hOBPs immobilized on the nanopores and the equivalent circuit, the diameter of semicircle at lower frequencies could be represented by half of the series impedance of R_p and R_{pore}, while that at higher frequencies was equal to half of R_{ct}, as shown in Fig. 3c. Hence, parameters of the parallel circuit could be extracted to analyze the impedance spectra of the interactions between ligands and the hOBPs functionalized nanopores.

3.2. Impedance detection of aldehydes and fatty acids

For aldehydes, especially aromatic aldehyde, they belong to volatile organic compounds that can be sensitively detected by human olfaction. Meanwhile, studies have been found that hOBPs have high affinities for aldehydes, such as benzaldehydes, which could be treated as the potential biomarkers of lung cancer and melanoma (Hanai et al., 2012; Kwak et al., 2013). In our study, benzaldehyde was chosen as one of the representative odorants and biomolecules for the impedance detection, firstly.

Under the treatment of benzaldehyde, the impedance spectra of the biosensor at lower frequencies changed obviously, while that at higher frequencies hardly changed, which indicated that interactions between hOBPs and benzaldehyde lead to the series impedance of R_p and R_{pore} to increase (Fig. 4a). As the concentrations of benzaldehyde increased from 10^{-8} mg/ml to 10^{-4} mg/ml, the series impedance of R_p and R_{pore} rose much obviously. Through calculating series resistances of R_p and R_{pore} of these different impedance spectra, we got the normalized impedance change (NIC) of benzaldehyde, which was described as $(Z_b - Z_a)/Z_b$, where Z_b and Z_a represent half of the series impedance of R_p and R_{pore} before and after benzaldehyde stimulation respectively. Though fitting the sigmoidal curve with a Hill equation, we got that the dissociation constant between hOBP and benzaldehyde was near 10^{-6} M. Moreover, NICs of benzaldehyde had a linear relationship with the logarithm of the concentrations from 10^{-8} mg/ml to 10^{-5} mg/ml, which was $y = 0.188 \log(x) + 1.732$ ($r^2 = 0.9542$), where x and y represent the concentrations of benzaldehyde and changes of NIC, respectively (Fig. 4b). The sensitivity was about $19\% \pm 3\%$ for every 10 mg/ml. Meanwhile, the detection limit was about 10^{-9} mg/ml. It suggested that interactions between hOBPs and benzaldehyde could be sensitively detected by the nanopore based impedance biosensor.

Besides aldehydes, hOBPs also showed high affinities to fatty acids, which have extensive metabolic, structural and functional roles within human bodies, such as modulating cellular signaling and interactions. Docosahexaenoic acid that contains 22 carbon atoms is one kind of omega-3 polyunsaturated fatty acid, which has a number of vital functions in vision, neuroprotection, and memory. Through detecting the impedance spectra of docosahexaenoic acid at different concentrations, the interactions

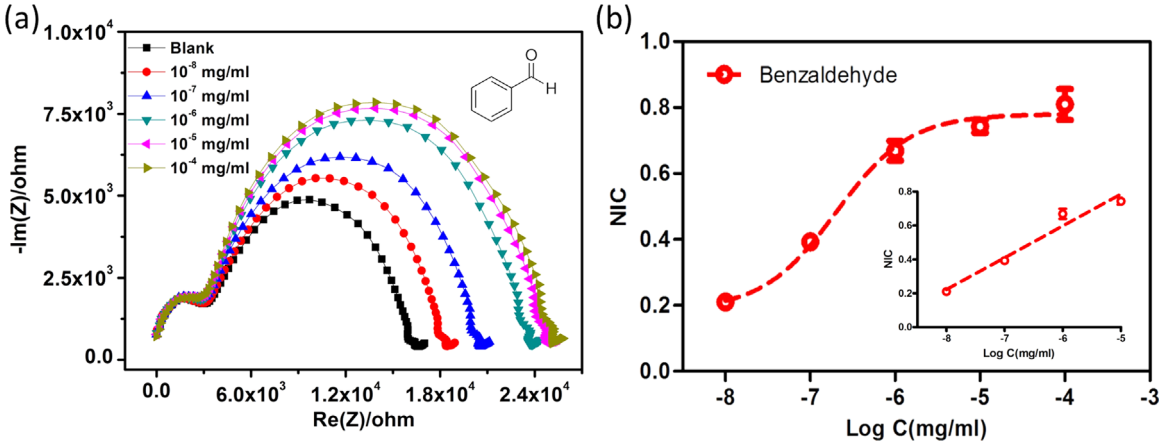

Fig. 4. Electrochemical detection for aldehydes: (a) impedance spectra of hOBPs to benzaldehyde from 10^{-8} mg/ml to 10^{-4} mg/ml and (b) normalized impedance changes (NICs) of hOBPs interacting with benzaldehyde (mean ± SD, $n=3$).

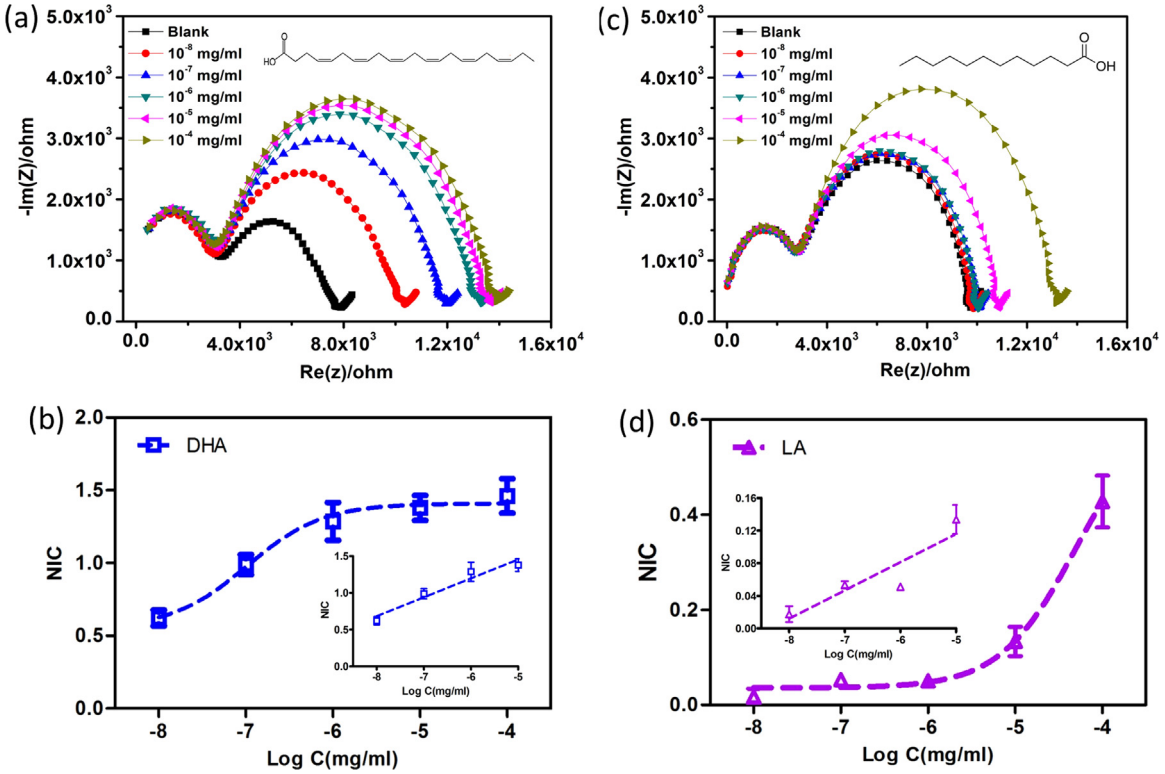

Fig. 5. Electrochemical detection for fatty acids: (a) impedance spectra of hOBPs to docosahexaenoic acid from 10^{-8} mg/ml to 10^{-4} mg/ml; (b) normalized impedance changes (NICs) of hOBPs interacting with docosahexaenoic acid that contains 22 carbon atoms; (c) impedance spectra of hOBPs to lauric acid from 10^{-8} mg/ml to 10^{-4} mg/ml and (d) NIC of hOBPs interacting with lauric acid that contains 12 carbon atoms.

between hOBPs and docosahexaenoic acid were also analyzed (Fig. 5a).

Similar to the impedance spectra of benzaldehyde, the series impedance of R_p and R_{pore} increased when the concentrations of docosahexaenoic acid were increasing. Moreover, from the sigmoidal curve of NICs from 10^{-8} mg/ml to 10^{-4} mg/ml, the dissociation constant between hOBP and docosahexaenoic acid was near 10^{-6} M (Fig. 5b). The best linear relationship with the logarithm of the concentrations was from 10^{-8} mg/ml to 10^{-5} mg/ml, which was $y=0.257\log(x)+3.896$ ($r^2=0.8891$). The sensitivity was about $26\pm6\%$ for every 10 mg/ml. Meanwhile, the detection limit was near 10^{-12} mg/ml. Therefore, this hOBPs functionalized biosensor provided a potential approach in docosahexaenoic acid detection with a high sensitivity.

Meanwhile, in order to detect affinities of hOBPs to fatty acids with different lengths of carbon chains, impedance spectra of lauric acid, which has 12 carbon atoms and belongs to medium-chain fatty acids, were detected (Fig. 5c and d). From 10^{-8} mg/ml to 10^{-4} mg/ml, the resistance changes were relatively low. The dissociation constant between hOBP and lauric acid was near 10^{-4} M. The linear relationship with the logarithm of the concentrations ranging from 10^{-8} mg/ml to 10^{-5} mg/ml was $y=0.035\log(x)+0.289$ ($r^2=0.7329$). The sensitivity was about $4\pm1\%$ for every 10 mg/ml. And, the detection limit was near 10^{-8} mg/ml. Compared to docosahexaenoic acid, lauric acid had a much less impact on the series impedance of R_p and R_{pore}, which indicated that interactions between hOBPs and lauric acid lead to small resistance changes of the protein. Moreover, the saturation concentration of lauric acid should be higher that 10^{-4} mg/ml.

Thus, the nanopore based biosensor showed a promising

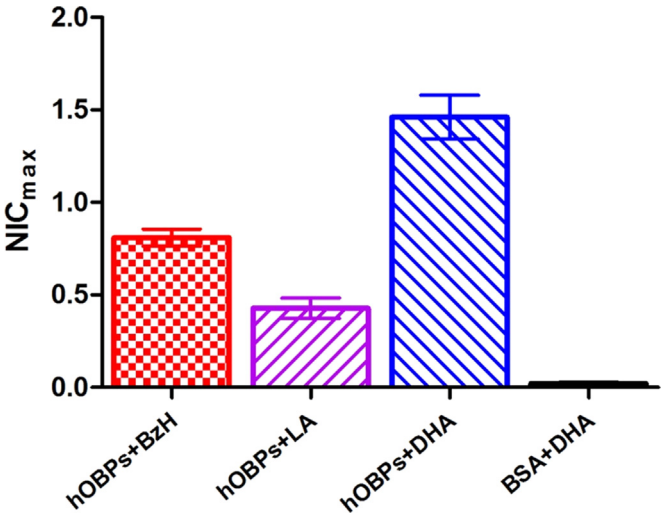

Fig. 6. Maximum NICs of hOBPs-modified nanopore arrays to benzaldehydes (BzH), lauric acid (LA), and docosahexaenoic acid (DHA), and BSA-modified nanopore arrays to DHA ($n=3$).

potential in discriminating fatty acids with different lengths of carbon chains, which was in accordance with that hOBPs might bind the larger chains more efficiently (Briand et al., 2002).

To examine that the impedance changes of hOBPs functionalized nanopores were caused by whether the attachment of proteins during measurements, or the different impedance of tested solution, BSA-modified nanopore arrays were also tested. Under the treatment of docosahexaenoic acid, resistance of nanopore arrays hardly changed, even at 10^{-4} mg/ml (Fig. 6). Thus, it demonstrated that impedance changes of hOBPs functionalized nanopores with addition of ligands should be generated from the specific binding of hOBPs and their ligands rather than other reasons.

In addition, to explore the odorant-binding properties of those ligands, the maximum values of NICs of the different ligands at 10^{-4} mg/ml were also compared (Fig. 6). There was a strong interaction between hOBPs and benzaldehyde, which could be reflected by the maximum changes of the normalized impedance (NIC_{max}), almost 80%. Through comparing NIC_{max} of benzaldehyde to lauric acid, however, it indicated that hOBPs had a relatively high affinity and sensitivity to benzaldehyde. With the number and length of carbon atoms of fatty acids increased, NIC_{max} increased. For docosahexaenoic acid, NIC_{max} at 10^{-4} mg/ml was near 150%, which was much larger than that of benzaldehyde and lauric acid. Therefore, hOBPs showed the highest affinity and sensitivity to docosahexaenoic acid in the tested ligands. These results validated that hOBPs-modified nanopores could mimic olfactory ability of human beings to a certain extent.

4. Discussion

4.1. hOBPs functionalized nanopore biosensor

As a cost-effective filtering membrane, nanopores were often employed in electrochemical testing as insulating membranes to stochastically sense (bio)molecules in solutions (Makra and Gyurcsányi, 2014). Functionalized with proteins that would be induced conformational changes by the corresponding testing substances, the detection signals of nanopores could be greatly amplified. Studies about OBPs showed that concerted dynamic phenomena might occur at the odorant entry site, which was likely related to the uptake–release mechanism of the ligands (Pelosi et al., 2005; Lescop et al., 2009). The conformational changes of OBPs had strong effects on electrical properties that could be detected by the nanopore based biosensors with quite special characteristics and relatively high sensitivities.

In this study, utilizing the conformation properties of hOBPs, an electrochemical impedance nanopore based biosensor was developed for both odorant and biomolecular ligand detection. When introducing nanopores into the three-electrode system, additional electron transfer process was induced. Before hOBPs immobilization, the characteristic resistance approximated half of R_{pore}. When the proteins were immobilized, a composite resistance–capacitance parallel circuit was introduced that changed the characteristic resistance into half of the series resistance of R_{pore} and R_p. More importantly, under the treatment of different ligands, only the series resistance of R_{pore} and R_p increased once again, which indicated that interactions between hOBPs and their ligands also increased the characteristic resistance of the hOBPs–nanopore complex.

4.2. Ligand detection with hOBPs based biosensor

As a volatile organic compound, benzaldehyde could be transported through liquid nasal mucus to make a sense of olfaction. Generally, aldehyde groups of benzaldehyde could interact with the lysine residues that located at the entrance and inside of the binding pocket of hOBPs, through hydrogen bonds, while the benzene rings of benzaldehyde could form π-stacking with other amino acids that contain benzene rings (Tcatchoff et al., 2006; Charlier et al., 2009). Additionally, the hydrophobic cavity of hOBPs had strong hydrophobic interactions with benzaldehyde. From the impedance spectra, it could be inferred that forming of the benzaldehyde–hOBP binding complex increased the resistance of proteins, and further influenced the whole impedance of the nanopores, while having little influence to the capacitance of hOBPs. Different from other benzaldehyde detection biosensors that based on insect ORs, and even antibodies, this impedance biosensor utilized hOBPs could provide a novel and sensitive platform for mimicking the human sense of smell to detect odorants (Gobi et al., 2007; Sato and Takeuchi, 2014; Onodera and Toko, 2014). More importantly, the good heat resistance and acid–base resistance properties of hOBPs made the nanopore based biosensor more robust to other biosensors utilized olfactory cells and ORs, which either needed strict experimental conditions or the protein expression and purification was often very difficult (Lee et al., 2012; Oh et al., 2014).

Fatty acids were crucial lipophilic biomolecules in the pathogenesis of numerous serious diseases, such as cardiovascular and neurodegenerative diseases, and even cancers (Bazan et al., 2011; Brasky et al., 2013). For the bindings between hOBPs and fatty acids, except for hydrogen bonds with lysine residues, other forces were also important, including hydrophobic interactions, and van der waals forces. Hence, fatty acids, especially those with long chains, could also change electrical properties of the hOBPs–nanopore complex. Thus, the hOBPs based biosensor that used nanopores had successfully detected fatty acids with different sensitivities. Compared to other kinds of biosensors, such as thermometric, piezoelectric, and optical biosensors, electrical biosensors with nanomaterials were regarded as strong candidates for rapid biochemical detections due to diagnosis without labeling steps, and compatibility with integrated circuits (Zhao et al., 2014; Roy et al., 2015). Although lacking of the real interference analytes that can also interact with hOBPs, the detection of different fatty acids would also be of immense significance not only in biomedical chemistry, but also in detecting biological molecules in serum and urine for diagnostic and pathological researches.

4.3. Applications of the hOBPs for biosensing

As one of the most important proteins in human olfaction, hOBPs play significant roles in regulating ingestive behavior, avoiding environmental hazards, and even chemical communication through transferring signals of outer world to human body. Meantime, serving for the transport, storage, or sequestration of a variety of small molecules, hOBPs exhibited good sensing properties. By directly targeting the sense of smell, this hOBPs functionalized nanopore biosensor could be used as an olfactory biosensor for special odorant detection, such as volatile odor biomarker detection.

What is even more amazing is that, except for identifying in nasal tissues to make sense of smell, hOBPs were also found as the extracellular carriers of lipophilic ligands in several other organs, such as lachrymal, prostate, and mammary glands (Schiefner et al., 2015; Schiefner and Skerra, 2015). Thus, hOBPs were found to be members of lipocalin superfamily and might be involved in various physiological processes, including fatty acid and pheromone signaling, immunomodulation, modulation of growth and metabolism, tissue development, and apoptosis. Learning from other human lipocalins, hOBPs could accommodate a myriad of biological signal molecules in various physiological processes. Therefore, through analyzing the interactions between hOBPs and their ligands, the hOBPs based nanopore biosensor offered an opportunity to investigate binding affinities of hOBPs to biomolecules *in vitro*. It also exhibited a promising potential in evaluating conditions of related organs, and even disease diagnosis through sensing and detecting important biomolecular ligands.

5. Conclusion

Based on conformation changes of hOBPs when binding to ligands and the sensing properties of nanopores, we have developed an electrochemical impedance biosensor for biochemical sensing. Through detecting benzaldehydes, docosahexaenoic acid, and lauric acid, which were closely related to cancers and other serious diseases, the hOBPs based biosensor showed specific characteristics. The detection limits of these three ligands were lower than 10^{-8} mg/ml. With the equivalent circuit of the biosensor, the interactions between hOBPs and different biomolecules were analyzed. The design of the hOBPs based biosensor provides a label-free platform for detecting odorants and important biomolecular ligands related to health. The sensor could be also used to explore the odorant-binding properties of hOBPs, and functions of hOBPs in different physiological processes.

Acknowledgments

This work was supported by the National Natural Science Foundation of China (Grant No. 81371643), the Zhejiang Provincial Natural Science Foundation of China for Distinguished Young Scholars (Grant No. LR13H180002), and the Research on Public Welfare Technology Application Projects of Zhejiang Province (Grant No. 2014C33149).

Appendix A. Supplementary material

Supplementary data associated with this article can be found in the online version at http://dx.doi.org/10.1016/j.bios.2015.12.047.

References

Albrecht, T., 2011. ACS Nano 5 (8), 6714–6725.
Bazan, N.G., Molina, M.F., Gordon, W.C., 2011. Annu. Rev. Nutr. 31, 321–351.
Bougnoux, P., Hajjaji, N., Maheo, K., Couet, C., Chevalier, S., 2010. Prog. Lipid Res. 49 (1), 76–86.
Brasky, T.M., Darke, A.K., Song, X., Tangen, C.M., Goodman, P.J., Thompson, I.M., Meyskens, F.L., Goodman, G.E., Minasian, L.M., Parnes, H.L., 2013. J. Natl. Cancer Inst. 105 (15), 1132–1141.
Briand, L., Eloit, C., Nespoulous, C., Bézirard, V., Huet, J.-C., Henry, C., Blon, F., Trotier, D., Pernollet, J.-C., 2002. Biochemistry 41 (23), 7241–7252.
Charlier, L., Cabrol-Bass, D., Golebiowski, J., 2009. C. R. Chim. 12 (8), 905–910.
Du, Z.-P., Wu, B.-L., Wu, X., Lin, X.-H., Qiu, X.-Y., Zhan, X.-F., Wang, S.-H., Shen, J.-H., Zheng, C.-P., Wu, Z.-Y., 2015. Sci. Rep. 5, 12010.
Garner, C.E., Smith, S., de Lacy Costello, B., White, P., Spencer, R., Probert, C.S., Ratcliffe, N.M., 2007. FASEB J. 21 (8), 1675–1688.
Gobi, K.V., Matsumoto, K., Toko, K., Ikezaki, H., Miura, N., 2007. Anal. Bioanal. Chem. 387 (8), 2727–2735.
Hanai, Y., Shimono, K., Oka, H., Baba, Y., Yamazaki, K., Beauchamp, G.K., 2012. Cancer Cell. Int. 12 (1), 7.
Hou, Y., Jaffrezic-Renault, N., Martelet, C., Tlili, C., Zhang, A., Pernollet, J.-C., Briand, L., Gomila, G., Errachid, A., Samitier, J., 2005. Langmuir 21 (9), 4058–4065.
Kaiser, L., Graveland-Bikker, J., Steuerwald, D., Vanberghem, M., Herlihy, K., Zhang, S., 2008. Proc. Natl. Acad. Sci. 105 (41), 15726–15731.
Kant, K., Yu, J., Priest, C., Shapter, J.G., Losic, D., 2014. Analyst 139 (5), 1134–1140.
Kwak, J., Gallagher, M., Ozdener, M.H., Wysocki, C.J., Goldsmith, B.R., Isamah, A., Faranda, A., Fakharzadeh, S.S., Herlyn, M., Johnson, A.C., 2013. J. Chromatogr. B 931, 90–96.
Lee, S.H., Jin, H.J., Song, H.S., Hong, S., Park, T.H., 2012. J. Biotechnol. 157 (4), 467–472.
Lescop, E., Briand, Lc, Pernollet, J.-C., Guittet, E., 2009. Biochemistry 48 (11), 2431–2441.
Liebes-Peer, Y., Rapaport, H., Ashkenasy, N., 2014. ACS Nano 8 (7), 6822–6832.
Lisdat, F., Schäfer, D., 2008. Anal. Bioanal. Chem. 391 (5), 1555–1567.
Liu, Q., Wang, H., Li, H., Zhang, J., Zhuang, S., Zhang, F., Hsia, K.J., Wang, P., 2013. Biosens. Bioelectron. 40 (1), 174–179.
Lu, Y., Li, H., Zhuang, S., Zhang, D., Zhang, Q., Zhou, J., Dong, S., Liu, Q., Wang, P., 2014. Sensors Actuators B: Chem. 193, 420–427.
Lu, Y., Yao, Y., Zhang, Q., Zhang, D., Zhuang, S., Li, H., Liu, Q., 2015. Biosens. Bioelectron. 67, 662–669.
Makra, I., Gyurcsányi, R.E., 2014. Electrochem. Commun. 43, 55–59.
Oh, E.H., Lee, S.H., Lee, S.H., Ko, H.J., Park, T.H., 2014. Biosens. Bioelectron. 53, 18–25.
Onodera, T., Toko, K., 2014. Sensors 14 (9), 16586–16616.
Pelosi, P., Calvello, M., Ban, L., 2005. Chem. Senses 30 (Suppl. 1), i291–i292.
Roy, P.K., Ganguly, A., Yang, W.-H., Wu, C.-T., Hwang, J.-S., Tai, Y., Chen, K.-H., Chen, L.-C., Chattopadhyay, S., 2015. Biosens. Bioelectron. 70, 137–144.
Santos, A., Kumeria, T., Losic, D., 2013. Trac. Trends Anal. Chem. 44, 25–38.
Sato, K., Takeuchi, S., 2014. Angew. Chem. Int. Ed. 53 (44), 11798–11802.
Schiefner, A., Freier, R., Eichinger, A., Skerra, A., 2015. Proteins: Struct. Funct. Bioinform. 83 (6), 1180–1184.
Schiefner, A., Skerra, A., 2015. Acc. Chem. Res. 48 (4), 976–985.
Schoch, R.B., Han, J., Renaud, P., 2008. Rev. Mod. Phys. 80 (3), 839–883.
Semin, G.R., De Groot, J.H., 2013. Trends Cognit. Sci. 17 (9), 427–429.
Stevenson, R.J., 2010. Chem. Senses 35 (1), 3–20.
Stoloff, D.H., Wanunu, M., 2013. Curr. Opin. Biotechnol. 24 (4), 699–704.
Tcatchoff, L., Nespoulous, C., Pernollet, J.-C., Briand, L., 2006. FEBS Lett. 580 (8), 2102–2108.
Tegoni, M., Pelosi, P., Vincent, F., Spinelli, S., Campanacci, V., Grolli, S., Ramoni, R., Cambillau, C., 2000. Biochim. Biophys. Acta—Protein Struct. Mol. Enzym. 1482 (1), 229–240.
Vitarelli Jr, M.J., Talaga, D.S., 2013. J. Chem. Phys. 139 (10), 105101.
Wei, R., Gatterdam, V., Wieneke, R., Tampé, R., Rant, U., 2012. Nat. Nanotechnol. 7 (4), 257–263.
Wei, Y., Brandazza, A., Pelosi, P., 2008. Biochim. Biophys. Acta—Proteins Proteom. 1784 (4), 666–671.
Zhao, Y., Deng, P., Nie, Y., Wang, P., Zhang, Y., Xing, L., Xue, X., 2014. Biosens. Bioelectron. 57, 269–275.